Vibration-assisted tunneling through competing molecular states

Katja C. Nowack and Maarten R. Wegewijs
Institut für Theoretische Physik - Lehrstuhl A , RWTH Aachen , 52056 Aachen , Germany
(Dated: March 23, 2022)

We calculate the non-linear tunneling current through a molecule with *two* electron-accepting orbitals which interact with an *intramolecular* vibration. We investigate the interplay between Coulomb blockade and non-equilibrium vibration-assisted tunneling under the following assumptions: (i) The Coulomb charging effect restricts the number of extra electrons to one. (ii) The orbitals are non-degenerate and couple asymmetrically to the vibration. (iii) The tunneling induces a non-equilibrium vibrational distribution; we compare with the opposite limit of strong relaxation of the vibration due to some dissipative environment. We find that a non-equilibrium *feedback* mechanism in the tunneling transitions generates strong negative differential conductance (NDC) in the model with two competing orbitals, whereas in a one-orbital model it leads only to weak NDC. In addition, we find another mechanism leading to weak NDC over a broader range of applied voltages. This pervasive effect is completely robust against strong relaxation of the vibrational energy. Importantly, the modulation of the electronic transport is based on an *intra*molecular asymmetry. We show that one can infer a non-equilibrium vibrational distribution when finding NDC under distinct gate- and bias-voltage conditions. In contrast, we demonstrate that any NDC effect in the one-orbital case is completely suppressed in the strong relaxation limit.

PACS numbers: 85.65.+h ,73.23.Hk ,73.63.Kv ,63.22.+m

arXiv:cond-mat/0506552v1 [cond-mat.mes-hall] 21 Jun 2005

Optical spectroscopy of vibrational modes has provided detailed information about the structure of molecules [1]. In a similar fashion, tunneling-current spectroscopy [2] may reveal microscopic details of single-molecule devices [3, 4, 5, 6, 7, 8]. At low temperature electrons tunneling onto a molecular device excite *discrete* vibrations by spending some of their excess energy provided by the bias voltage. The resulting changes in the current with bias voltage are determined by the effective potentials for the nuclear vibration in different *charge* states, in contrast to optical spectroscopy. This provides information on how the molecule is situated in a nanojunction (center of mass modes between the electrodes) [4] and the role of different parts of the molecule in the transport (internal modes) [5, 6, 8]. It is also of interest to *control* the electronic response of molecular devices by designing their mechanical properties through chemical synthesis. In this respect, the center of mass modes of a molecule in a nanojunction are less attractive since they are difficult to tailor and most sensitive to relaxation through interaction with the surface of the junction electrodes [9, 10]. Internal modes of a molecular device, in contrast, are expected to remain more discrete. They reflect more intrinsic properties of the device amendable to chemical engineering. Recently, the coupling of such a tailored mode to the tunneling transport has been experimentally investigated in a C_{140} fullerene-dimer [5]. In view of the ongoing experimental efforts, it is of interest which current-spectroscopic features of a molecular device distinguish vibrational excitations from electronic ones.

Theoretical works have already addressed several issues in the weak tunneling limit by focusing on a one-orbital model including the Coulomb blockade effect and coupling to a single localized vibration. At finite bias voltage the electron tunneling will tend to drive the vibration out of equilibrium [11, 12, 13, 14]. Several mechanisms may reduce the accumulated vibrational energy: coupling to the environment [9], the tunneling itself [13, 14, 15] and also intramolecular vibrational energy redistribution due to anharmonic mode coupling. The effects of the renormalization of the tunneling by Franck-Condon (FC) factors on the vibrational distribution were discussed in detail [13]. These factors incorporate the effect of the change in the nuclear configuration when changing the electronic state and charge of the molecule. In the limit of strong electron-vibration coupling current suppression and a related super-poissonian current noise were predicted as well as a weak NDC effect [15, 16]. Strong NDC effects [12] were found by assuming the electron-vibration coupling to increase with bias voltage. Finally, in the strong tunneling limit a Kondo effect due to charge (instead of spin) fluctuations was discussed for strong coupling to the vibration [17, 18].

In this paper we consider a molecule with *two* electron-accepting orbitals coupled to a single internal vibration with frequency ω. We consider the weak tunneling limit $\Gamma \ll T$ where Γ is the typical tunneling rate to the electrodes and T the electron temperature. The strong Coulomb charging effect is assumed to restrict the number of electrons which can be added to the molecule to one. This introduces a competition between vibration-assisted tunneling processes associated with the different orbitals. We focus on the case where the orbitals are non-degenerate (splitting Δ) and asymmetrically coupled to the vibration (couplings $\lambda_1 \neq \lambda_2$). Additionally, we assume that the vibrational distribution on the molecule can be driven out of equilibrium (no relaxation). For comparison we also discuss the technically simpler limit of strong relaxation. Due to the asymmetric coupling to the vibration the bare *electronic* splitting is renormalized to the observable splitting Δ which we will consider

as an effective parameter. We find that negative differential conductance (NDC) effects are enhanced compared with the one-orbital case and actually dominate the transport. Basically, the orbital coupled stronger to the vibration contributes little to the transport but functions as a trap due to a *feedback* mechanism in the tunneling transitions. The competing weakly coupled orbital gives the main contribution to the current but at the same time enhances the feedback by providing an additional path to the trap. Several types of features appear: (i) Franck-Condon progressions of alternating conductance resonances and *anti-resonances* resulting in *current oscillations* which are robust against strong relaxation; (ii) anomalous *current peaks* of width $\propto T$ due to a strongly bias dependent redistribution of vibrational energy; (iii) isolated gate- and bias- voltage regions outside of which the current is strongly suppressed due to a stabilization of the charged state which couples stronger to the vibration. (iv) when the excited orbital couples stronger to the vibration a voltage-controlled *population inversion* between the two charged electronic states takes place which is signalled by NDC occuring at special resonances. Importantly, the effects are based on the Coulomb blockade and the intramolecular asymmetry (non-degenerate electronic states and asymmetric coupling to the vibration). No asymmetric electronic wave function overlap with the electrodes needs to be assumed (similar to the NDC induced by to spontaneous emission [19]). This offers the interesting perspective of designing electronic transport properties of a molecular device by synthetic control of the electro-mechanical aspects. We note that for a related model of two degenerate orbitals current rectification was predicted assuming strong relaxation [20]. There the asymmetric coupling to the electrodes is essential.

The paper is organized as follows. In Section I we introduce the two-orbital model and the master equations for the molecular state occupancies. We discuss the qualitative dependence of the FC-factors on the vibrational numbers and show that the Condon-parabola from optical spectroscopy is also a useful tool in transport-spectroscopy. In Section II A we first discuss the NDC effect noted in Ref. [15] for the one-orbital model and relate it to the feedback mechanism. We then exhaustively discuss the effect of this mechanism for the two-orbital case in the limits where one orbital couples weakly to the vibration: $\lambda_1^2 > 1 \gg \lambda_2^2$ (Section II B) and $\lambda_1^2 \ll 1 < \lambda_2^2$ (Section II C). In Section II D we illustrate how the mechanism leads to more complex results for asymmetric strong coupling $\lambda_1^2 \neq \lambda_2^2 > 1$. We present a comprehensive overview and discussion in Section III.

I. MODEL

Molecule. We consider the minimal model $H = H_M + \sum_r H_r + H_T$ incorporating the molecule (M), the electrodes $r = L, R$ and the tunneling (T) in units $\hbar = k_B = 1$:

$$H_M = \sum_i (\epsilon_i n_i + u_i n_\uparrow n_\downarrow) + v n_1 n_2 + \frac{\omega}{2}\left[P^2 + \left(Q - \sum_i \sqrt{2}\lambda_i n_i\right)^2\right], \quad (1)$$

$$H_r = \sum_{ki\sigma} \epsilon_{kr} a^\dagger_{k\sigma r} a_{k\sigma r}, \quad (2)$$

$$H_T = \sum_{ki\sigma r} t_{ir} a^\dagger_{k\sigma r} c_{i\sigma} + h.c.. \quad (3)$$

The Hamiltonian H_M describes a molecule with two electron-accepting orbitals $i = 1, 2$ (operators $c_{i\sigma}$, energies ϵ_i) with an energy splitting $\Delta = \epsilon_2 - \epsilon_1$. Here $n_i = \sum_\sigma n_{i\sigma}$, $n_{i\sigma} = c^\dagger_{i\sigma} c_{i\sigma}$. We assume throughout that double occupation of each orbital is completely suppressed due to strong local Coulomb interactions u_i i.e. $n_i \leq 1$. Simultaneous occupation of the two orbitals is similarly suppressed by the interaction v which introduces an important correlation: $\sum_i n_i \leq 1$. Since u_i and v are the largest energy scales they do not enter explicitly in any further way. The nuclear configuration of the molecule is assumed to be altered with respect to some coordinate Q when either orbital is occupied. The effective potentials for the nuclear motion in these charged states (here in the harmonic approximation, frequency ω) are shifted relative to the neutral state by $\sqrt{2}\lambda_i, i = 1, 2$. The coordinate $Q = (b + b^\dagger)/\sqrt{2}$ is normalized to the nuclear zero-point motion by $(M\omega)^{-1/2}$ (M = nuclear mass involved) and λ_i is dimensionless. Here $b^\dagger$ excites the vibrational mode by one quantum ω and $P = (b - b^\dagger)/\sqrt{2}i$ is the conjugate nuclear momentum. The energy scale characterizing the electron-vibration coupling associated with orbital $i = 1, 2$ is the change in the elastic energy at fixed nuclear configuration $\omega\lambda_i^2$. Vibration-assisted processes are thus expected to lead to a progression of conductance resonances spread over a bias voltage range of at least $\sim \max\{\lambda_i^2\omega\}$. Typical energies ω of internal vibrations observed experimentally range up to a few tens of meV [4, 5, 6, 7, 8]. In general electron-vibration coupling is expected to be particularly strong for many-particle states of molecules which are characterized to a good approximation by occupation of a particular orbital [21], which is typically the case for charged states of otherwise neutral molecules. Large relative displacements $|\lambda_i| > 1$ of the nuclear potentials may be expected, for instance, when Q is an angle coordinate and the nuclear configuration of the charged molecule is internally twisted relative to the neutral one [22].

The electronic energy parameters in Eq. 1 are the relevant effective parameters for finite λ_i. These are related to their values for $\lambda_1 = \lambda_2 = 0$ (indicated by a superscript (0)) by $\epsilon_i = \epsilon_i^{(0)} - \lambda_i^2\omega, u_i = u_i^{(0)} - 2\lambda_i^2\omega, v = v^{(0)} - 2\lambda_1\lambda_2\omega$. This is seen by diagonalizing the molecular Hamiltonian through a translation of the nuclear coordinates [23], $U = \prod_{i=1,2} e^{-\lambda_i n_i (b^\dagger - b)}$. The resulting

Hamiltonian has the form (1) where $\lambda_i, i = 1, 2$ is eliminated. The electron becomes "dressed" with vibrational excitations (polaron) resulting in the renormalization of the energy parameters which we anticipated in writing Eq. 1. The renormalization of the charging energies is irrelevant here since we assume them to be largest energy scales (i.e. $u_i^{(0)} \gg 2|\lambda_i|^2\omega, i = 1, 2$ and $v^{(0)} \gg 2|\lambda_1\lambda_2|\omega$). The correlations $n_1 + n_2 \leq 1, n_i \leq 1$ are thus not weakened. Cases where a strong renormalization of the interaction becomes relevant were discussed in [17, 18]. In contrast to the one-orbital model the renormalization of the orbital energies is important when the coupling to the vibration is asymmetric, $\lambda_1 \neq \lambda_2$. Then the electronic splitting is renormalized to an effective value $\Delta = \epsilon_2 - \epsilon_1 = \Delta^{(0)} + \omega(\lambda_1^2 - \lambda_2^2)$ which can even have a different sign as $\Delta^{(0)}$. Since only the excitation energy Δ is observable in the transport characteristics, we use it as an independent positive parameter i.e. the state 1 by definition has the lowest renormalized energy ϵ_1. We are interested in the case where resonances related to orbital and vibrational excitations occur on the same voltage scale, i.e. $\omega \sim \Delta \lesssim \max\{\lambda_i^2\omega\}$. The transport mechanism which we wish to illustrate operates in the limit of asymmetric coupling. This requires that either the lowest orbital couples strongly to the vibration or the excited orbital, see Fig. 1. We point out that in Hamiltonian (1) we have not written intramolecular terms which couple the two nuclear potentials 1 and 2. Such terms become important, for instance, when the electronic energy splitting is an integer multiple p of the vibrational energy quantum, $\Delta = p\omega$. This has been discussed in Ref. [20] for the case $\Delta = 0$ and $\lambda_1 = -\lambda_2$. Here we avoid such degeneracies, i.e. we assume $t \ll min_p\{\Delta - p\omega\}$, where t is a tunneling amplitude between the electronic states. Furthermore, we can safely disregard electronic transitions induced by the nuclear motion near the crossing of the potentials 1 and 2 since for large asymmetric coupling the barrier separating the minima of potentials $i = 1, 2$ is $(\Delta/\omega(\lambda_1 - \lambda_2)^{-1} \pm (\lambda_1 - \lambda_2))^2\omega/4 \gg \omega$. Below we will also present results for cases of moderate asymmetry of the vibrational couplings where such effects may start to play a role. These will serve as a simple starting point for the discussion of the strong asymmetry case and also illustrates the enhancement of NDC effects when multiple orbitals (instead of just one) are competing in the transport.

The electrodes $r = L, R$ are modeled by H_r, Eq. (2), as non-interacting quasi-particle reservoirs at electrochemical potential μ_r. The electrode-molecule tunneling H_T, Eq. (3), picks up the shift of the nuclear coordinate from the unitary transformation of the molecular operators: $H_T = \sum_{ki\sigma r} t_{ir} a_{k\sigma r}^\dagger e^{-\lambda_i(b^\dagger - b)} \bar{c}_{i\sigma} + h.c.$ Here $\bar{c}_{i\sigma}^\dagger$ creates a polaron state associated with the effective potential of electronic orbital $i = 1, 2$. Since we consider here an intramolecular vibration we do not include a dependence of the bare tunneling matrix elements t_{ir} on the coordinate Q (shuttle-effect, cf. Ref. [12, 24]).

Master equations. We are interested in the weak tunneling regime, $\Gamma \ll T$, where in addition the vibrational excitations can be resolved, $T \ll \omega$. We can describe the transport using diagonal density matrix elements P_q^i (occupation probabilities, $\sum_{i=0}^{2}\sum_q P_q^i = 1$) , where $q = 0, 1, 2, \ldots$ is the vibrational number and $i = 1, 2$ denotes the charged state with only orbital i occupied and the neutral state is labeled by $i = 0$. The transitions including the vibrational excitations q, q' are denoted by $0_q \leftrightarrows 1_{q'}$ and $0_q \leftrightarrows 2_{q'}$. The occupation probabilities are coupled by the stationary master equations

$$\begin{aligned} \dot{P}_q^0 = 0 &= \sum_i \sum_{rq'} \left(W^r_{0q \leftarrow iq'} P^i_{q'} - 2W^r_{iq' \leftarrow 0q} P^0_q \right), \\ \dot{P}_q^i = 0 &= \sum_{rq'} \left(2W^r_{iq \leftarrow 0q'} P^0_{q'} - W^r_{0q' \leftarrow iq} P^i_q \right), \end{aligned} \tag{4}$$

where $i = 1, 2$, with transition rates ($f_r(\epsilon) \equiv (e^{(\epsilon - \mu_r)/T} + 1)^{-1}$)

$$\begin{aligned} W^r_{iq' \leftarrow 0q} &= \Gamma^{ri}_{qq'} f_r(\mu^i_{q'-q}), \\ W^r_{0q \leftarrow iq'} &= \Gamma^{ri}_{qq'} (1 - f_r(\mu^i_{q'-q})). \end{aligned} \tag{5}$$

The addition energies for the transition $i_{q'} \leftarrow 0_q$ are

$$\mu^i_{q'-q} = \epsilon_i + (q' - q)\omega - \alpha V_g. \tag{6}$$

The gate voltage V_g effectively varies μ relative to the ground-state transition energy μ_0^1 ($\alpha =$ capacitance ratio) and the bias voltage $V > 0$ is applied symmetrically, $\mu_{L,R} = \mu \pm V/2$. The stationary current flowing out of reservoir $r = L, R$ is given by ($I_L + I_R = 0$)

$$I_r = \sum_{qq'} \sum_i \left(2W^r_{iq \leftarrow 0q'} P^0_{q'} - W^r_{0q \leftarrow iq'} P^i_{q'} \right). \tag{7}$$

The equations for the one-orbital case with coupling λ_1 are obtained by simply discarding all $P^2_{q'}$ in Eqs. (4) and (7) and are equivalent to those in Refs. [11, 12, 13, 14, 15]. The current will change whenever a line in the (μ, V) plane is crossed corresponding to a right-electrode

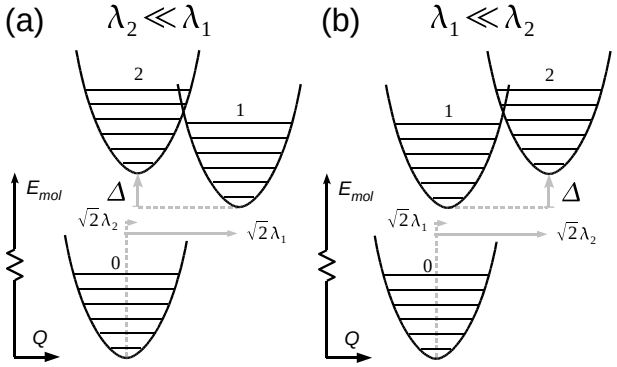


FIG. 1: Schematic effective nuclear potentials for neutral ($i = 0$) and charged ($i = 1, 2$) electronic states of molecule. (a) Strongly coupled ground state (b) Strongly coupled excited state.

resonance $\mu_R = \mu^i_{q'-q}$ (positive slope in (μ, V) plane) or a left-electrode resonance $\mu_L = \mu^i_{q'-q}$ (negative slope). Importantly, due to the harmonic excitation spectrum only the *change* in vibrational number $q'-q$ enters in the resonance condition: transitions between all states $i_{q'}$ and 0_q with fixed difference $q'-q$ become allowed at a single resonance. A *cascade* of single-electron transitions can then lead to a significant population of high vibrational excitations, e.g. $i_0 \to 0_0 \to i_1 \to 0_1 \to i_2 \to 0_2 \to \cdots$ is a possible cascade for $\mu_L > \mu^i_1 > \mu^i_0 > \mu_R$.

Franck-Condon factors and Condon parabola. The tunneling rates consist of two factors: $\Gamma^{ri}_{qq'} = \Gamma^{ri} F^i_{qq'}$. The tunneling rates $\Gamma^{ri} = 2\pi|t_{ir}|^2\rho_r$ between electrode $r = L, R$ (density of states ρ_r) and orbital $i = 1, 2$ determine the overall current scale. The FC factors $F^i_{q'q} = F^i_{qq'}$ take into account that the stable nuclear geometry is changed when occupying orbital i:

$$F^i_{qq'} = |\langle q|X_i|q'\rangle|^2 = e^{-\lambda_i^2}\frac{q!}{q'!}\lambda_i^{2|q-q'|}\left(L_q^{|q-q'|}(\lambda_i^2)\right)^2, \quad (8)$$

where L is the associated Laguerre-polynomial and $q < q'$. Note that the sign of λ_i does not play a role. The general sum rule $\sum_q F^i_{qq'} = \sum_{q'} F^i_{qq'} = 1$, guarantees that the current will saturate at large bias voltage to the value it would have without the vibrations ("electronic limit"). This holds *only* when the λ_i do not depend strongly on the bias voltage (cf. [12]).

Without vibrations, asymmetry of the tunneling rates with respect to the orbital- and electrode- index gives rise to NDC [25] and super-poissonian current noise [26], see also [27, 28, 29]. Below we show that qualitatively different dependence of the FC factors $F^i_{qq'}$ on the vibrational numbers for state $i = 1, 2$ and the effective energy splitting Δ give rise to NDC effects which can dominate the transport. We therefore set $\Gamma^{ir} = \Gamma, i = 1, 2, r = L, R$ and restrict our discussion to $V > 0$ since in this case $I(-V) = -I(V)$. We symmetrize the stationary current $I = (I_L - I_R)/2$ and decompose it into a sum of positive partial currents of the states weighted with their occupation:

$$I = \sum_q I^0_q P^0_q + \frac{1}{2}\sum_i \sum_{q'} I^i_{q'} P^i_{q'} \quad (9)$$

$$I^0_q = \Gamma \sum_{q'}\sum_i F^i_{qq'}\left(f_L(\mu^i_{q'-q}) - f_R(\mu^i_{q'-q})\right) \quad (10)$$

$$I^i_{q'} = \Gamma \sum_q F^i_{qq'}\left(f_L(\mu^i_{q'-q}) - f_R(\mu^i_{q'-q})\right) \quad (11)$$

For low $T \ll \omega$ the partial currents are the FC factors $F^i_{qq'}$ summed over the transitions $0_q \leftrightarrows i_{q'}$ inside the bias window $\mu_L > \mu^i_{q'-q} > \mu_R$ in Fig. 2. Note that the partial current of the neutral state I^0_q has contributions from both charged states $i = 1, 2$ into which it can decay. One can understand the numerical results in almost all detail using the following simple graphical scheme. This approach works for multiple orbitals and also for a more general shape of the nuclear potential. Without going into the details, we comment on the basic points in the procedure. In Fig. 2 the FC factor associated with the transition between a pair of states $0_q \leftrightarrows i_{q'}$ is depicted as function of q and q'. The change in the partial currents in (9) with increasing bias can be understood by drawing the bias voltage window in this figure. Only qualitative features of the FC factors are of importance which follow from simple quasi-classical arguments. The FC-factor $F^i_{qq'}$ is basically non-zero only in the classically allowed region delimited by the tilted *Condon parabola* [1]:

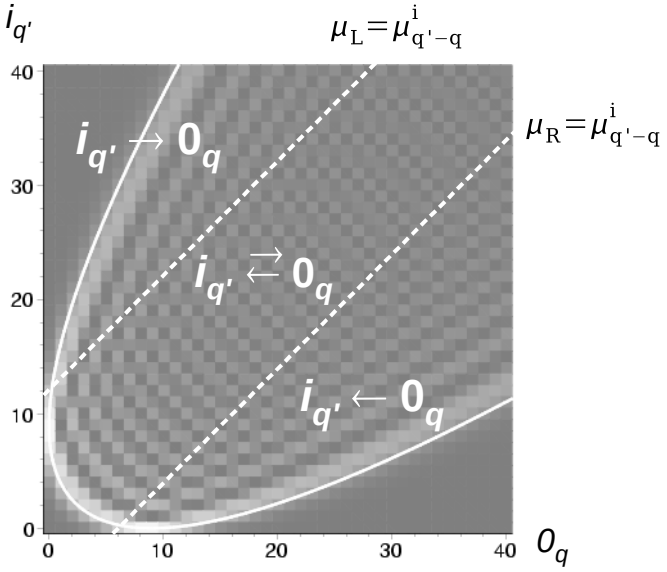


FIG. 2: Franck-Condon factors $F^i_{qq'}$ in linear grey-scale (white = positive, gray=zero) for a transition between $i_{q'}$ and 0_q involving a strong relative displacement $\lambda_i = 3$. The Condon-parabola Eq. 12 (white full line) separates the classically forbidden and allowed regions. The partial current $I^i_{q'}/\Gamma$, Eq. (11), is obtained by adding the FC-factors for transitions in the bias window (strip of width and height V/ω between the dashed white lines) horizontally for fixed q'. The partial current I^0_q/Γ, Eq. (10) is obtained similarly by adding the FC-factors in this strip vertically for fixed q and adding the contributions from both states $i = 1, 2$.

$$q + q' \geq \frac{|q-q'|^2}{\lambda_i^2} + \frac{\lambda_i^2}{2} \quad (12)$$

In this region the classical orbits of the nuclear motion in the shifted potentials intersect in phase-space. The FC-factor oscillates with q, q' with a quasi-classical envelope which varies algebraically on the scale of λ_i^2 [30]. The global maxima $\approx 1/\lambda_i^2$ are attained where the parabola touches the axes ($q \approx \lambda_i^2, q' = 0$ and $q = 0, q' \approx \lambda_i^2$). In the classically forbidden region where the opposite of condition (12) holds the FC factor $F^i_{qq'}$ is exponentially small. In the forbidden regions where $q' \gg q$ or $q' \ll q$ the nuclear momenta of the two motions are incompatible. These regions exist for any value of λ_i. Starting from the allowed region the FC-factors eventually decrease exponentially with increasing q' or q. On the other hand,

the forbidden region where $q, q' \ll \lambda_i^2$ is only well defined for $\lambda_i^2 \gg 1$. In this case $F^i_{qq'}$ initially *increases exponentially* with increasing q' or $q \ll \lambda_i^2$. This "inverted" regime exists for nuclear potentials of more general shape with large relative displacements of the potential minima. As the bias window in Fig. 2 widens, the partial currents increase. For weak coupling $\lambda_i^2 \ll 1$ the Condon-parabola is very narrow i.e. transitions which conserve the vibrational number have the largest amplitude. When the bias window reaches the vertex of this narrow parabola nearly all partial currents reach their maximal value at once. For strong coupling, $\lambda_i^2 \gg 1$, the parabola is very broad and the partial currents show a slow exponential increase as the bias window widens. The complex transport characteristics of the two orbital model considered here follow from two intramolecular asymmetries between the orbitals: (1) the bias window covers different parts of the Condon-parabola due to the electronic splitting Δ and (2) the Condon-parabolas are qualitatively different due to asymmetric coupling to the vibration.

Strong relaxation. We now prove an important restriction on the occurrence of NDC in the limit where the vibrational excitations completely relax before each tunneling event due to some dissipative environment. This limit implies the factorization ansatz $P^i_q = P^i P_q$ with the vibrational equilibrium distribution $P_q = e^{-q\omega/T}(1 - e^{-\omega/T})$. We can then reduce the equations (4) to an effective electronic three-level problem with effective bias-voltage dependent rates (cf. [10, 13]) obtained by averaging over the equilibrium distribution:

$$W^r_{0\leftarrow i} = \sum_{qq'} W^r_{0q\leftarrow iq'} P_{q'}, W^r_{i\leftarrow 0} = \sum_{qq'} W^r_{iq\leftarrow 0q'} P_{q'} \quad (13)$$

(these vary monotonically with V) and $W_{0\leftarrow i} = \sum_r W^r_{0\leftarrow i}$,$W_{i\leftarrow 0} = \sum_r W^r_{i\leftarrow 0}$. The stationary current in electrode $r = L, R$ reads ($I_L + I_R = 0$):

$$I_r = 2\frac{\sum_i \left(W^r_{i\leftarrow 0} - W^r_{0\leftarrow i}\frac{W_{i\leftarrow 0}}{W_{0\leftarrow i}}\right)}{1 + 2\sum_i \frac{W_{i\leftarrow 0}}{W_{0\leftarrow i}}}. \quad (14)$$

In Appendix A we show that in this case for two orbitals the current can be reduced by increasing the bias voltage at resonances related to the *left electrode*, $\mu_L = \mu^i_k, k = 1, \ldots$ (for $V > 0$), i.e. lines with positive slope in the (μ, V) plane. Here the transition $i_{q+k} \leftarrow 0_q$ becomes allowed. Any NDC along a resonance line with positive slope is thus a *proof of a non-equilibrium vibrational distribution* on the molecule. For one orbital the current can never decrease with V in this limit. Finally, we consider the limit where in addition to the strong relaxation, the transitions $0_q \leftrightarrows i_{q'}$, $i = 1, 2$ are not correlated i.e. the renormalized Coulomb interaction [17, 18] is zero: $v' = 0$. It is readily shown (Appendix B) that in this case the current increases monotonically with bias voltage for *any number* of orbitals. The strong Coulomb correlations are thus essential for NDC effects.

Intermediate relaxation. Basically all the physics is captured by considering the opposite limits of negligible and strong relaxation. We have confirmed this by considering intermediate regimes where we add a relaxation term $\sum_{q'} W_{q\leftarrow q'} P^i_{q'}$ to the right-hand side of the equation for $\dot{P}^i_q$, Eq. (4). We considered an environment [11] with either ohmic ($s = 1$) or sub-ohmic ($s = 0$) spectral function $J(E) = \gamma|E/\omega|^s$ for which the relaxation rates are $W_{q\leftarrow q'} = J(\omega(q - q'))[\pm N(\omega(q - q'))]$ for $q \gtrless q'$ where $N(E) = (e^{\beta E} - 1)^{-1}$. We briefly discuss the results for intermediate relaxation when interesting deviations from a simple interpolation between non-equilibrium and strong relaxation limit occur.

II. RESULTS

We now present results for the stationary current I (Eq. (7)) and differential conductance dI/dV for symmetric tunneling rates $\Gamma^{ir} = \Gamma, r = L, R, i = 1, 2$. Throughout the paper we set the temperature to $T = 0.025\omega$. Gray-scale plots of $dI/dV(\mu, V)$ have been given different linear scale factors for $dI/dV \gtrless 0$ to clarify the voltage conditions under which NDC occurs. The NDC magnitude can be inferred from the presented $I(V)$ curves. We note that the results for a molecule with two neutral states and one charged state are simply obtained by inverting the sign of $\mu - \mu^1_0$ and modifying the discussion accordingly.

A. Strongly coupled single orbital - Feedback mechanism and weak NDC

In Ref. [15] the one-orbital model in the limit of strong coupling to the vibration ($\lambda_1^2 \gg 1$) was shown to exhibit a current suppression which was related to "avalanches" of vibration assisted tunneling processes which also leads to super-poissonian current noise effects [15, 16]. Additionally, for asymmetric gate voltages a weak NDC effect was noted in the absence of relaxation. Here we focus on this weak NDC effect and additional small current *peaks* (not discussed in Ref. [15]) which are visible in Fig. 3 as black lines and white-black double lines, respectively. The mechanism responsible for this is based on an energy asymmetry (induced by the gate potential) and the qualitative features of the FC-factors. This mechanism will also play a role in the transport involving two (or more) orbitals where it results in much stronger effects. We therefore consider this simple case in some detail.

Current suppression. The differential conductance plotted in Fig. 3 is symmetric about $\mu = \mu^1_0$ up to unimportant differences in amplitude due to spin degeneracy of the orbital (without which we would have exact symmetry) so we only discuss the case $\mu \geq \mu^1_0$; the opposite case follows from interchanging the roles of the electronic states $0 \leftrightarrow 1$. For low voltages $V \ll 2\omega\lambda_1^2$ states with low vibrational number are predominantly occupied and the current is exponentially suppressed both in the limit of weak and strong relaxation [15, 16]. This is related

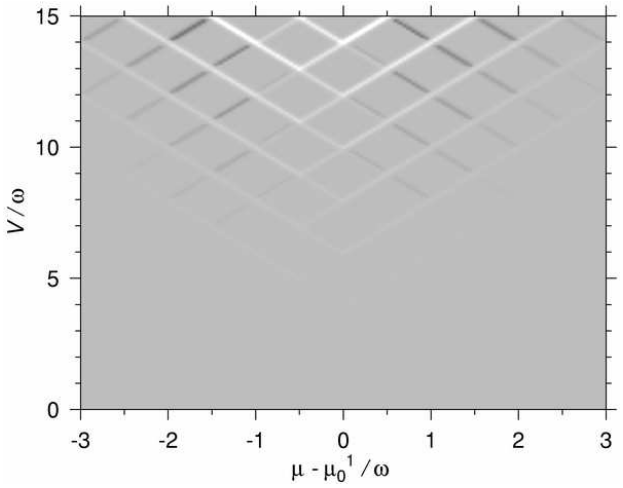


FIG. 3: One-orbital model with strong electron-vibration coupling $\lambda_1 = 5.0$. Differential conductance in gray-scale (gray: $dI/dV = 0$, white / black: $dI/dV \gtrless 0$) as function of bias V and gate voltage μ.

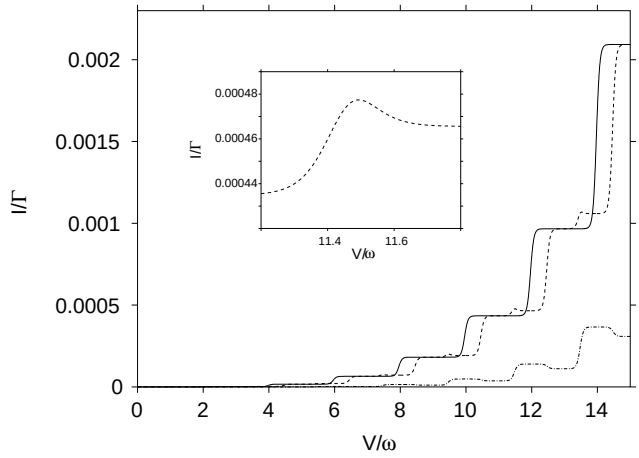


FIG. 4: Current-voltage characteristics for increasing $\mu - \mu_0^1 = 0\omega, 0.25\omega, 1.75\omega$ (going down) in Fig 3 for non-equilibrium vibrations (Eq. (7)). Inset: small current peak for $\mu - \mu_0^1 = 0.25\omega$ which for larger $\mu - \mu_0^1$ develops into a current drop.

to the classically forbidden region $q, q' \ll \lambda_1^2$ in Fig. 2 where the FC factors depend exponentially on the vibrational numbers. In the limit of strong relaxation the current suppression is simply due to the exponentially small partial currents of the few vibrational states which are thermally occupied at low $T \ll \omega$. In the absence of relaxation the FC-factors also prevent the excited states from actually becoming occupied for $V \ll 2\omega\lambda_1^2$. The resulting non-equilibrium vibrational distribution induced by the tunneling is "equilibrium-like" as was noted before [13, 15]. This is due a type of *feedback* mechanism in the tunneling transitions, as we will now explain. In principle at finite bias voltage arbitrarily high vibrational excitations can be accessed via *cascades* of single-electron

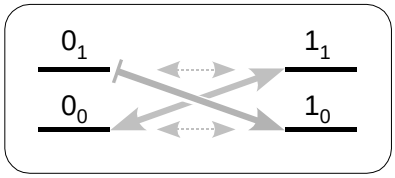


FIG. 5: Relevant transitions for Fig. 3. For clarity only vibrational energy differences are indicated. For $\mu > \mu_0^1$ a *feedback* cascade of transitions keeps the state 1_0 nearly fully occupied leading to NDC and current peaks.

tunneling processes. However, at low bias voltage transitions which lie outside the bias window in Fig. 2 (i.e. $0_q \to 1_{q'}$ resp. $0_q \leftarrow 1_{q'}$) correspond to large changes of the vibrational energy and have exponentially larger rates. Once the initial states for these transitions start to be occupied, the total rate for populating the lowest states (transitions outside the bias window) becomes much larger than the total rates of its decay (transitions inside bias window). As a result only the low-lying states are occupied due to the large asymmetry between the rates. Compared with the strong relaxation limit vibrational excitations are slightly more favored and therefore the current suppression is less severe [15] in this limit (not shown). The central observation is that although the occupations decrease strongly with vibrational number this is compensated by the exponential increase of the partial currents. The *main* contribution to the current comes from the excited states. The "inverted" dependence of the FC-factors on energy (vibrational numbers) thus stabilizes the lowest vibrational state and enhances the sensitivity of the current to the small occupations of the vibrational excitations. This is at the basis of the weak NDC and small current peaks which we will discuss now.

Weak NDC and current peak. Apart from the quantitative effect on the current suppression, there appear interesting qualitative new features in the absence of relaxation. The many visible resonance lines in Fig. 3 form a *Franck-Condon progression* which extends beyond voltages $\sim 2\omega\lambda_1^2$. Interestingly, for asymmetric gate energy $\mu - \mu_0^1 > \omega/2$ the current can be reduced at the resonances $\mu_L = \mu_k^1, k = 1, 2, \ldots$ (black features on right in Fig. 3). Here the transitions $0_q \to 1_{q+k}, q = 0, 1, \ldots$ become allowed and one could naively expect the current to increase since this favors the population of the excited states $1_{q+k}, q > 0$ which are responsible for the main current contributions. Actually, the opposite happens. Due to the asymmetric gate-energy $\mu - \mu_0^1 > 0$ a *feedback* mechanism is active which involves a cascade of single-electron transitions. This is illustrated in Fig. 5. In the regime of voltages where NDC occurs the charged vibrational ground state 1_0 is stabilized, not only relative to the neutral states (due to the Coulomb blockade) but also relative to the vibrationally excited charged states $1_q, q > 0$. Due to the asymmetric gate energy state 1_0 has less transitions which depopulate it than which pop-

ulate it, see Fig.5. Due to the strong increase of the FC-factors with vibrational number this asymmetry in the rates causes a nearly complete occupation of 1_0 for asymmetric gate energies. Upon increasing the bias, at resonances where the excitations 1_{q+k} become accessible other excitations $0_{q'}$ with $q' \approx q + k$ are also favored via subsequent tunneling processes involving small changes in the vibrational number. These subsequent transitions are allowed already at low V. The excitations $0_{q'}$ decay with large rates back to the the state 1_0 and its first few excitations, since they change the vibrational number by a large amount. Importantly, the reverse of the latter transition, $0_{q'} \leftarrow 1_0$ is not allowed at low T, see Fig. 5. Therefore the occupation of 1_0 is effectively increased at the expense of the excited states which contribute most to the current and NDC occurs.

Small current peaks of width $\propto T$ occur in the intermediate region $0 < \mu - \mu_0^1 \lesssim \omega/2$ (white-black double lines in Fig. 3 and inset of Fig. 4). These signal a redistribution of the vibrational energy when the bias is tuned through the resonance. In this case the above feedback mechanism can only become effective when the transition energy lies sufficiently close to μ_L. Thus initially the current rises but once the excited states become sufficiently populated they start to relax via the feedback and the current drops again.

Finally, Fig. 4 shows that even though the absolute current-step amplitude exponentially increases with increasing bias voltage [15], the NDC becomes relatively less pronounced. Careful inspection reveals that at sufficiently large gate energy $|\mu - \mu_0^1|$ the resonances initially correspond to current drops but with increasing voltage turn into peaks and finally become current steps. The increasing bias eventually compensates for the gate-asymmetry and the feedback mechanism becomes ineffective.

In the limit of strong relaxation at low $T \ll \omega$ only transitions inside the bias window along the $q = 0$ and $q' = 0$ axis in Fig. 2 play a role (cf. Eq. 13). The charged vibrational ground state is stabilized due to a gate voltage $\mu - \mu_0^1 > 0$ and the strong relaxation. However, no NDC or current peaks can occur at the resonances discussed above since the vibrational distribution is not affected by the tunneling in this limit. The feedback mechanism is cut off: after each single-electron tunneling process the excitation relaxes on a much shorter time scale and the next tunneling process starts from a vibrational ground-state again. Indeed one can show explicitly that in the limit of complete relaxation the NDC and the current peaks disappear in the one-orbital model for arbitrary spin and orbital degeneracy (see Appendix A). We note that at resonance lines $\mu_R = \mu_{-k}^1$ for $k = 1, 2, \ldots$ the current always increases, independent of the relaxation. Here the transitions $1_q \to 0_{q+k}$ become allowed whereby 1_0 can decay and repopulate the excited states which carry the current.

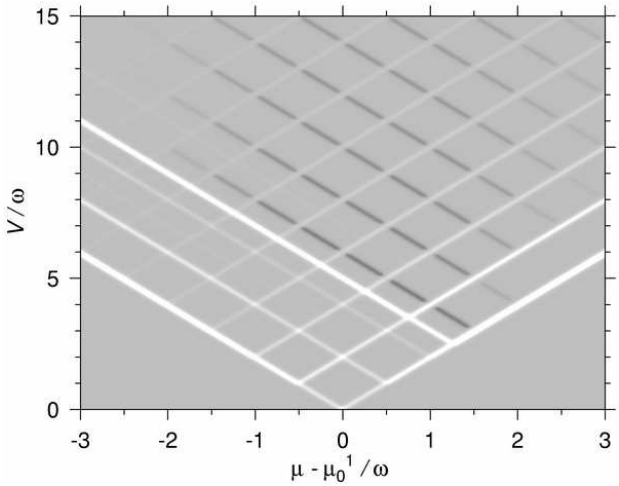


FIG. 6: Differential conductance $dI/dV(\mu, V)$ for $\lambda_1 = 1.4$, $\lambda_2 = 0.1$, $\Delta/\omega = 2.5$. Current steps (white lines with negative slope) due to stronger coupled orbital 1 become current *drops* (dark lines) as soon as the weakly coupled orbital 2 contributes to the current.

B. Strongly coupled ground state

We now demonstrate that in a two-orbital model with asymmetric coupling to the vibration already at moderate coupling a new but weak NDC effect occurs which is robust against strong relaxation, in contrast to the weak NDC in the one-orbital model. Additionally, the non-equilibrium feedback mechanism responsible for the weak NDC in the one-orbital model leads to strong NDC effects for two competing orbitals. These general statements carry over to the case of multiple non-degenerate orbitals with asymmetric coupling occupied by at most one electron due to Coulomb blockade. We start our discussion with an intermediate case where only the weak NDC occurs.

1. $\lambda_1^2 \gtrsim 1 \gg \lambda_2^2$ *Weak NDC - Current oscillations*

The differential conductance and typical I-V curve in Fig. 6 and 7, respectively, display a number of features which can be understood by considering the two orbitals invidually. Vibrational excitations of the stronger coupled state 1 form a FC progression of resonances far beyond $V \approx 2\lambda_1^2\omega$. In contrast, the excitations of the weakly coupled orbital 2 only show up as a single dI/dV peak at $\mu_L = \mu_0^2$. The resonances $\mu_L = \mu_k^1$ of the stronger coupled state 1, correspond to current steps for $k \leqslant [\Delta/\omega]$. Interestingly, once the weakly coupled state 2 has started to contribute to the current, $\mu_L > \mu_0^2$, these turn into *anti-resonances*, $k > [\Delta/\omega]$, (dark lines in Fig. 6 with negative slope). The resonances, $\mu_R = \mu_{-k}^1, k \geq 0$, always correspond to current steps (white lines in Fig. 6 with positive slope). A distinctive feature is that the current steps and drops due to the excitations of the

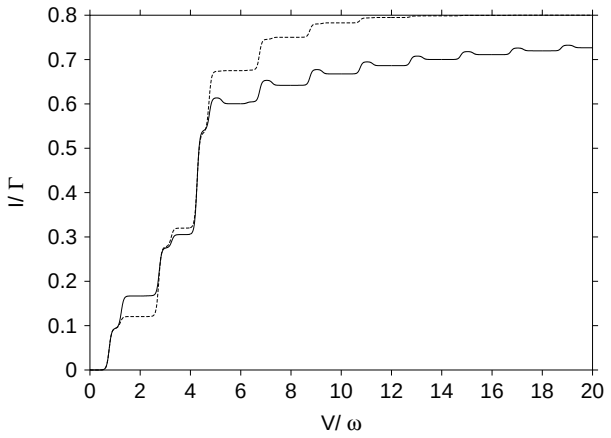


FIG. 7: Current-voltage characteristic for $\mu - \mu_0^1 = 0.375\omega$ in Fig. 6 for non-equilibrium (full, Eq. (7)) and equilibrium vibrations (dashed, Eq. (14)). The oscillatory pattern of current steps and drops sets in only when orbital 2 contributes to the current (here $V > 5.0\omega$).

stronger coupled state have opposite gate voltage dependence. Since they are of the same order of magnitude they give rise to current *oscillations* on the slowly saturating background. We note that for identical parameters the one-orbital model (i.e. with either $\lambda_1 = 0.1$ or 1.4) produces negligible NDC effects. The origin of the enhancement of NDC is the following. For moderate gate energy $\mu - \mu_0^1$ the partial currents of states 1_q are small compared with those of states 2_q and 0_q, cf. Fig. 2. At resonance lines $\mu_L = \mu_k^1$ the transitions $1_{q+k} \leftarrow 0_q$ become allowed, and the occupations of the states with the larger partial currents are reduced due to the Coulomb correlation between the two orbitals. The asymmetry between the partial currents is only present when the weakly coupled orbital 2 is accessible, therefore the current drops at these resonances only once both orbitals are accessible, i.e. $\mu_L \geqslant \mu_0^2 \geqslant \mu_R$. In contrast, the resonances $\mu_R = \mu_{-k}^1, k > 0$ correspond to current steps since here states 1_q are depopulated in favor of the states with larger partial currents.

Although the current oscillations in Fig. 6 seem very similar to those for the one-orbital model in Fig. 3, there is an important difference: here the NDC is not completely suppressed in the strong relaxation limit, although larger values of the dominant coupling λ_1 are required for visibility comparable with the limit of no relaxation. In Appendix A we prove that in the strong relaxation limit a drop of the current can only occur along resonance lines $\mu_L = \mu_k^i$ (negative slope) if it occurs. A condition for the visibility of NDC is that the total current below the resonance is larger than compared with the partial current of the orbital causing it. This requires a weakly coupled orbital, $\lambda_2^2 \ll 1$, with large partial currents in combination with a stronger coupled orbital, $\lambda_1^2 \gtrsim 1$. These are roughly the same conditions as for the visibility of the oscillating current in the non-equilibrium limit. However, we point out that under identical bias and gate voltage conditions the NDC need not to be visible in both the non-equilibrium and equilibrium limit, see for instance Fig. 7 and Fig. 10 below.

In summary, the current oscillation occurs due to the competition between transport channels with significantly different partial currents. It is a *Coulomb repulsion* effect: the current calculated without the effective correlations ($v = 0$), always increases with V (see Appendix B).

2. $\lambda_1^2 \gg 1 \gg \lambda_2^2$ *Strong NDC*

When the charged ground state couples strongly to the vibration , $\lambda_1^2 \gg 1$, and the electronic excitation lies low, $\Delta < \omega$, we find the typical structure of Fig. 8. The current oscillations are clearly visible again and this set of resonances needs no further discussion. An obvious difference with Fig. 6 is the finite gap $\geq \Delta$ for any gate voltage. In fact, in addition to the Coulomb blockade regime where $\mu_L < \mu_0^1$ or $\mu_0^1 < \mu_R$ resp., the current is suppressed in the entire strip $\mu_0^2 \geq \mu_L \geq \mu_0^1, \mu_R > \mu_0^1$ (i.e. where the excited orbital 2 is not yet accessible). This is due to the exponentially small FC-factors $F_{qq'}^1, q, q' \ll \lambda_1^2$ of the lowest orbital which now couples strongly to the vibration (cf. Sec. II A). When increasing the bias voltage above the gap the resulting current depends strongly on the order in which additional transitions become allowed i.e. on the gate voltage. Basically four different situations can occur which are labeled (a)-(d) in Fig. 8 and the relevant transitions are schematically indicated in Fig. 9.

(a) Stabilization of the charged ground state. In the upper-right region in Fig. 8, the current may be expected to flow: the transitions $2_{q'} \leftrightarrows 0_q$ are energetically allowed for at least $q = q' = 0$, for which the FC-factor is large, $F_{00}^2 \approx 1$. Instead the current is strongly suppressed and increases in small steps of increasing height with increasing bias. This is very similar to the situation in Fig. 4 where the transport is dominated by a single orbital with $\lambda_1^2 \gg 1$. Between states $1_{q'}$ and 0_q the feedback mechanism discussed in Sec. II A is operative which keeps state 1_0 almost fully occupied with increasing bias, see Fig. 9(a) and compare with Fig. 5. The presence of orbital 2 further enhances the feedback since the states 0_q (which feed back into 1_0) can now also be populated via cascades of transitions involving orbital 2.

(b,c) Isolated region. The small diamond-shaped region in Fig. 8 at *finite voltage* $\Delta < V < 2\omega$ is remarkable. Inside it the current is non-zero and beyond any of its four defining boundaries in the plane of gate- and bias voltage the current is completely suppressed. A typical $I(V)$ curve through this region is shown in Fig. 10. The fact that the region is bounded by a *NDC line with positive slope* proves that it must be caused by non-equilibrium vibrational effects (Sec. I), see also the strong relaxation result in Fig. 10. This region can be reproduced by truncat-

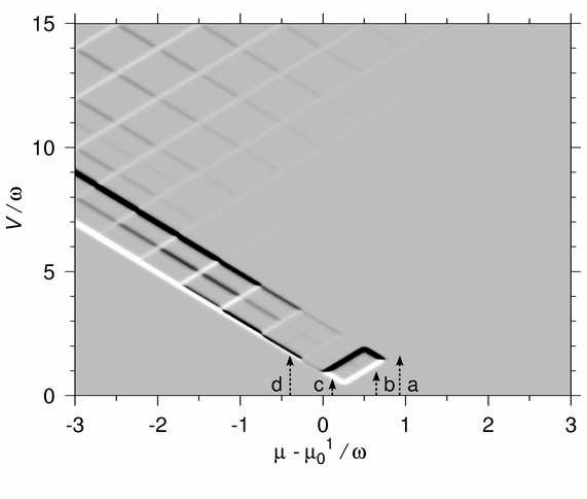


FIG. 8: $dI/dV(\mu, V)$ for $\lambda_1 = 5$, $\lambda_2 = 0.1$ and $\Delta/\omega = 0.5$. The isolate region at low bias is due to the small excitation energy $\Delta < \omega$ and disappears for $\Delta > \omega$. The current is strongly suppressed once the *weakly coupled* state 2 can be excited, $\mu_L > \mu_1^2$ and $\mu_R < \mu_{-1}^2$ (thick black lines). A current *peak* (white-black double line) appears when this orbital becomes accessible at $\mu_L = \mu_0^2$.

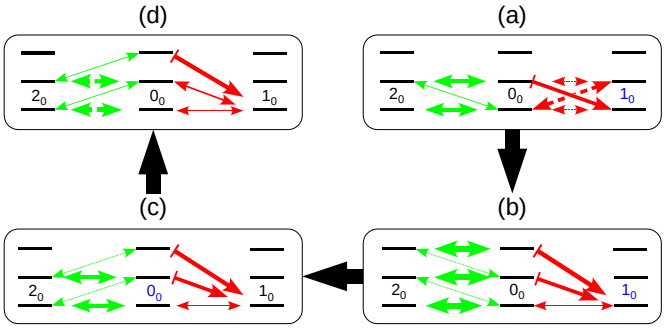


FIG. 9: Relevant transitions in low bias section of Fig. 8. Indicate are transitions which cause NDC to occur when increasing the bias along (a)-(d). For clarity only vibrational energies are indicated. Arrow thicknesses indicate relative magnitude of the transition rates between vibrational excitations of a pair of states $0_q \leftrightarrows i_{q'}, q, q' = 0, 1, 2, \ldots$ where $i = 1$ or $i = 2$. Rates between different pairs of states are of different order of magnitude since different couplings (λ_1 or λ_2) is involved. The cascades of transitions give rise to a *feedback* into the lowest vibrational state 1_0 of strongly of the coupled orbital.

ing the spectrum to 5 states: $0_q, 2_q, q = 0, 1$ and 1_0, see also Fig. 9. At the low bias side, Coulomb blockade and the small FC factor F_{00}^1 discussed above are responsible for the current suppression. Inside this region only the transitions $2_0 \leftrightarrows 0_0 \leftrightarrows 1_0$ are allowed. The stationary occupations follow from Eq. (4): $P_0^0 = 1/5, P_0^1 = P_0^2 = 2/5$ and the current is:

$$I \approx \frac{1}{2} I_0^2 P_0^2 + I_0^0 P_0^0 = \frac{2}{5}\Gamma \qquad (15)$$

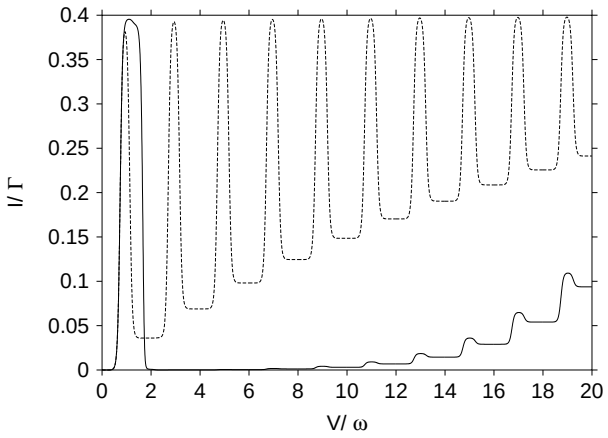


FIG. 10: $I(V)$ for $\mu - \mu_0^1 = 0.375\omega$ in Fig. 8 [case (b)], for non-equilibrium (full, Eq. (7)) and equilibrium vibrations (dashed, Eq. (14)). The isolated current plateau at low bias $V \leq 2\omega$ and the subsequent current suppression are non-equilibrium effects. For this gate energy both the current oscillations and the rising background current are *enhanced* when one allows for strong relaxation (in contrast to the one-orbital model).

This is less than $2\Gamma/3$ and $4\Gamma/5$, the maximal current through one and two orbitals (without the vibration), respectively, due to the partial occupation of the strongly coupled state 1_0 with suppressed partial currents. Note that state 1_0 is not yet blocking the transport. At the high bias side, the current becomes suppressed when the first neutral excited state 0_1 can be reached either via the cascade $0_0 \to 2_1 \to 0_1$ (NDC line with negative slope, case (b) in Figs. 8 and 9) or $2_0 \to 0_1$ (NDC line with positive slope, case (c)). State 0_1 can decay to 1_0 when an electron enters the molecule through *either* junction i.e. the reverse transition $0_1 \leftarrow 1_0$ is suppressed at low temperature $T \ll \omega - \Delta$. Now state 1_0 is almost fully occupied since it is populated much faster than it can decay: it is blocking the transport since the current it limited by the very small sum of its decay rates. The feedback loop thus involves both the weakly and strongly coupled state: the competition between the two orbitals which couple asymmetrically to the vibration causes the NDC to be much stronger compared with the one-orbital case (Sec.II A). From the above it follows that the diamond-shaped region disappears for excitation energy $\Delta > \omega$. However, the feature (a) and (d), which we discuss now, will still be present.

(d) Current peak. At the resonance line $\mu_L = \mu_0^2$ where the weakly coupled orbital 2 starts to participate a single large current step could be expected. Remarkably, NDC occurs *in the middle* of this resonance, producing a *current peak* (white-black double line with negative slope in Fig. 8) whose width is proportional to the electron temperature T. This sharp features stands out between the thermally broadened plateaus in Fig. 11. The origin of the peak is a strong competition between the charged states 1_0 and 2_0 in the narrow energy window

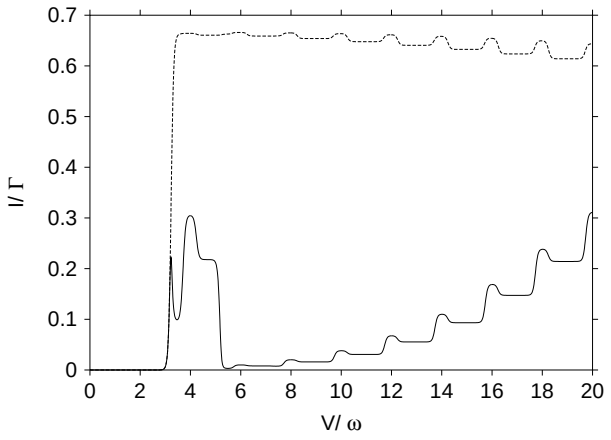


FIG. 11: $I(V)$ for $\mu - \mu_0^1 = -1.125\omega$ in Fig. 8 [case (d)] for non-equilibrium (full, Eq. (7)) and equilibrium vibrations (dashed, Eq. (14)). The current sets on with a *peak* of width $\propto T$, the other local maxima are thermally smeared plateaus. The downward trend of the equilibrium curve only applies at low voltages $V < 2\lambda_1^2\omega$, it saturates to the "electronic limit" at larger voltages.

$|\mu_L - \mu_0^2| \sim T$, involving the feedback via neutral excited states 0_q. This is most simply illustrated by considering gate energies $\Delta/2 - \omega < \mu - \mu_0^1 < \Delta/2 - \omega/2$ where a minimal set of 6 states is sufficient to understand the peak, see Fig. 9(d). At the rising side of the peak the rate of the transition $2_0 \leftarrow 0_0$ (through the V dependence in the Fermi-function, cf. Eq. 5) has increased sufficiently to enhance the current relative to the very small value supported only by the transitions to / from the blocking state, $1_0 \leftrightarrows 0_0$. Due to the gate energy the simplest feedback loop involves a cascade of 6 transitions: $0_0 \to 2_0 \to 0_1 \to 2_1 \to 0_2 \to 1_0$. This feedback initially remains ineffective since the excited state 0_2 is not yet sufficiently populated. The vibrational distribution is equilibrium-like and the current follows the result for equilibrated vibrations, see Fig. 11. As one increases V the occupations of the excited states in the feedback loop increases and a maximum is reached. Here the feedback dynamically starts to trap the molecule in the state 1_0. The occupations of the excited states and the current now start to decrease and reach a lower value (although higher than before the peak). The current peak thus signals this redistribution of the vibrational energy in a small bias window. We note that the current is not completely suppressed: this only happens beyond the second strong NDC line $\mu_L = \mu_1^2$ (cf. Fig. 11) as may be understood by considering Fig. 9(d). The peak can thus be considered a precursor of the full onset of the feedback mechanism. For lower $\mu - \mu_0^1 < \Delta/2 - \omega$ a similar argument involving more than 6 states explains why the peak becomes a step and why simultaneously the strong NDC along $\mu_L = \mu_1^2$ is further enhanced.

Intermediate relaxation. Upon increasing the vibrational relaxation rate γ (cf. Sec. I) starting from zero, the strong relaxation result is approached as expected. The relaxation cuts off the cascade of transitions leading to the blocking state and reduces the importance of the feedback for the transport. Now the NDC becomes more pronounced at resonances $\mu_L = \mu_k^1, k = 1, 2, ...$ where the transitions $0_q \to 1_{q+k}$ become allowed. These enhance the occupation of 1_0 due to relaxation and suppress the current. However, this approach is rather slow at low bias voltages: the NDC lines marking the isolated region remain clearly visible.

In summary, the strong NDC lines $\mu_L = \mu_1^2$ and $\mu_R = \mu_{-1}^2$ are associated with excitations of the state with *weakly* coupled to the vibration (state 2). However, the *strongly* coupled state 1 is actually blocking the transport. The weakly coupled state allows an excess vibrational energy to accumulate on the molecule (through a cascade of tunneling processes) which is subsequently spent to trap the molecule in the strongly coupled state (in a single tunneling process). The blocking state can thus be reached under very general energetic conditions. Therefore NDC effects become strong when 2 (or more) orbitals which couple asymmetrically to the vibration compete in the transport. Finally we note that Fig. 8 is reminiscent of the signatures of spin-blockade of tunneling. There the resonance line marking the transition between ground states can be terminated at finite bias and the current is only recovered when excited states become accessible [31]. The resonance line thus shows a kink. Here the kink in the resonance line is more drastic since also transitions to *many* vibrationally excited states are suppressed. Such details are of importance to distinguish NDC due to spin excitations in molecules [32] from effects due to vibrational excitations.

C. Stronger coupled excited state

We now consider the case opposite to Section II B where the excited orbital 2 takes up the role of the blocking orbital due to a strong(er) coupling to the vibration and the lower orbital 1 is weakly coupled. Vibration-assisted tunneling processes now stabilize the electronically excited state of the charged molecule i.e. an *excess charge and energy* may be stored on the molecule by the feedback mechanism. We focus on the resulting qualitative differences with respect to Sec. II B resulting from this population-inversion controlled by the bias voltage. As a simple reference point, we start again from an intermediate case.

1. $\lambda_1^2 \ll 1 \lesssim \lambda_2^2$ *Weak NDC - current oscillations*

Fig. 12 shows the typical differential conductance for $\Delta > \omega$. Similar to Fig. 6 the weakly coupled state (state 1) basically shows up as one large current step and the many resonance lines correspond to the excitations of the strongly coupled state (here state 2). However, at

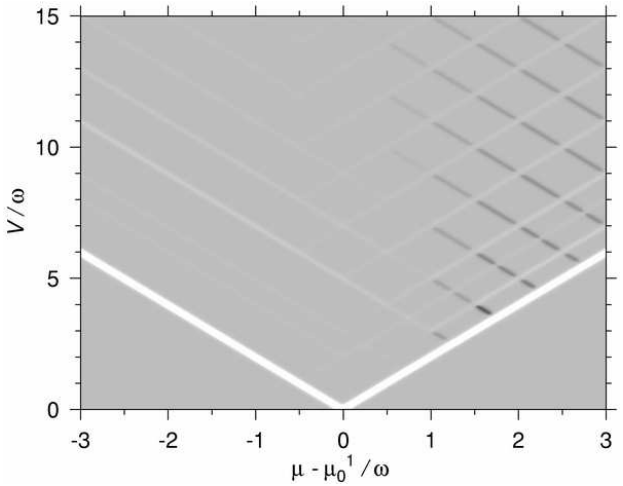


FIG. 12: $dI/dV(\mu, V)$ for $\lambda_1 = 0.1$, $\lambda_2 = 1.4$, and $\Delta/\omega = 2.5$. The oscillations are similar to those in Fig.12. The current drops (black lines with negative slope) are again due to the *stronger* coupled orbital 2.

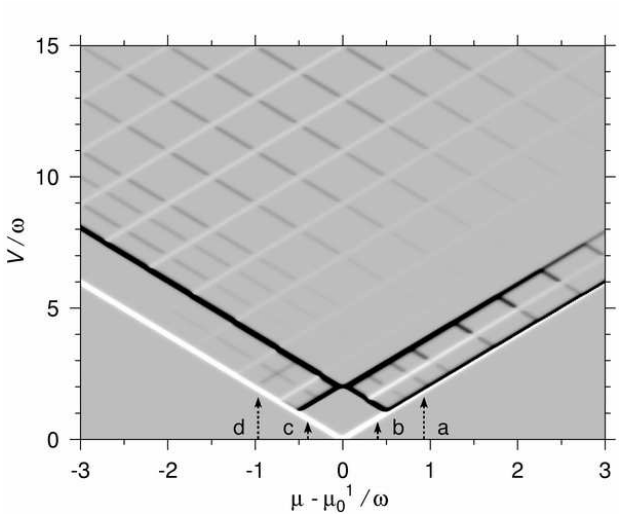


FIG. 13: $dI/dV(\mu, V)$ for $\lambda_1 = 0.1$, $\lambda_2 = 5.0$, and $\Delta/\omega = 2.5$. Similar to Fig. 8 a two strong NDC lines define a low bias structure and a current *peak*, which now occurs at $\mu > \mu_0^1$. The progression of NDC lines extending up to large bias voltage is again due to the strongly coupled *excited* orbital 2. Remarkably, this NDC already sets in at low V, before this orbital can be directly accessed: this signals *absorption* of vibrational energy by *incoming* electrons.

the resonances $\mu_L = \mu_k^2, k \geq [\Delta/\omega]$ we have current drops for small $|\mu - \mu_0^2|$ (i.e. away from the charge degeneracy point) and current steps for large $|\mu - \mu_0^2|$. Therefore, around the charge degeneracy point $\mu = \mu_0^1$ the first few excitations beyond the electronic excited line $\mu_L = \mu_0^2$ show up as current steps and only at higher bias voltage turn into current drops, in contrast to the case where the lower orbital couples stronger to the vibration (Fig. 6). Up to now we have only found features in the differential conductance (either positive or negative) when incoming electrons excite the vibration with their excess energy. This is expected at low temperatures $T \ll \omega$. Interestingly, in Fig. 12 a small current step at the resonance $\mu_L = \mu_{-1}^2$ with negative slope is visible which corresponds to *absorption* of the vibrational energy by an *incoming* electron despite the low temperature $T \ll \omega$ and moderate bias. The slightly enhanced current may be understood as an effect of significant heating of the molecule by the vibration assisted-tunneling.

2. $\lambda_1^2 \ll 1 \ll \lambda_2^2$ *Strong NDC*

When the coupling to the charged excited state becomes strong, $\lambda_2^2 \gg 1$ the case of most interest is that of a higher excited orbital, $\omega < \Delta \ll \lambda_2^2\omega$. The typical structure is shown in Fig. 13. In contrast to Fig. 8 we do not have a gap here since the change in the nuclear configuration of the two ground states is now small: the current starts to flow at the edges of the Coulomb blockade region $\mu_L = \mu_0^1$ and $\mu_0^1 = \mu_R$. Two NDC lines stand out in Fig. 13 (dark) where the current is significantly suppressed: $\mu_L = \mu_1^1$ and $\mu_R = \mu_{-1}^1$. Again, the appearance of the latter NDC line with positive slope is a proof that non-equilibrium vibrations play a role (Sect. I). At these lines the transitions $1_{q+1} \leftarrow 0_q$ and

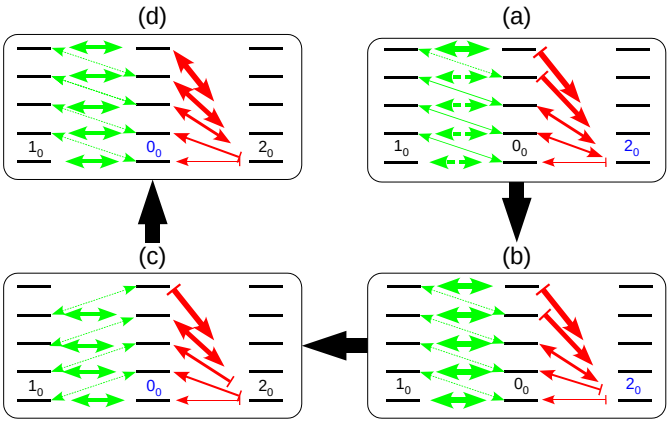


FIG. 14: Same diagram as Fig. 9 but now for low-bias section of Fig. 13. The feedback mechanism now involves more excitations $0_q, 1_q, q \leq \Delta/\omega > 1$. Note the state which is stabilized by this non-equilibrium mechanism , 2_0, is an *electronically* excited state i.e. we have a population inversion.

$1_q \rightarrow 0_{q+1}$ between the neutral and the *weakly* coupled charged state become allowed which enhance the occupation of the excited states 0_q. The latter feed back to the strongly coupled state 2_0 with rates which increase exponentially with q and the electronic excited orbital is predominantly occupied. We thus have a bias-controlled *population inversion* between ground- and excited state of the charged molecule due to their asymmetric coupling to the vibration. We discuss the four different situations labeled (a)-(d) in Fig. 13 for which the relevant transitions are schematically indicated in Fig. 14.

(a) Current peak. A current *peak* appears along the line $\mu_R = \mu_0^1$ for $\mu - \mu_0^1 > \omega/2$ (white-black double line on the right in Fig. 13). Compared with Fig. 8 this peak occurs on the opposite side and remains visible up to much higher values of $\mu - \mu_0^1$. The mechanism causing the current peak is analogous to that discussed in Section II B 2 with the roles of 1 and 2 interchanged. However, more vibrational excitations are involved in the feedback mechanism depicted in Fig. 14 since $\Delta > \omega$. For moderate gate energy $\mu - \mu_0^1$ the current peak is a precursor to the population inversion: the feedback is only completely activated beyond the resonance above it, $\mu_R = \mu_{-1}^1$. There the transitions $1_q \to 0_{q+1}$ become allowed and the strongly coupled state 2_0 is predominantly occupied suppressing the current (upper-right region in Fig. 13). For large asymmetric gate energy $\mu - \mu_0^1 \gg \omega/2$ the peak actually *marks* the population inversion: the NDC at the peak gains in amplitude at the expense of the NDC above it at $\mu_1^1 = \mu_R$ (opposite to Fig. 8). In this case state 2_0 can already be reached by many feedback cascades $0_0 \to 1_k \to 2_0, 1 \le k \le [(\mu - \mu_0^1)/\omega]$, once the escape from orbital 1 ($0_0 \leftarrow 1_0$) becomes possible. Therefore the population inversion and current suppression are complete at the peak. For a low-lying excited orbital, $\Delta < \omega$, this is in fact the general situation since the cascade of transitions involved in the feedback is shorter.

(b,c) Isolated region. For $|\mu - \mu_0^1| < \omega/2$ and $V < 2\omega$ we have an isolated region in the sense that the current reaches a local maximum value (diamond shaped region at bottom of Fig. 13). This region does not occur for $\Delta < \omega$ (opposite to Sec. II B 2 where $\Delta > \omega$ suppresses the isolated region). Within this region only the transitions $1_0 \leftrightarrows 0_0$ are allowed, $P_0^0 = 1/3, P_0^1 = 2/3$, and the current

$$I \approx I_0^0 P_0^0 + \frac{1}{2} I_0^1 P_0^1 = \frac{2}{3}\Gamma \tag{16}$$

equals the maximum current which a single orbital (without the vibration) can carry. When going along (b) and (c) in Fig. 13 we next cross the resonance lines $\mu_L = \mu_1^1$ and $\mu_R = \mu_{-1}^1$ respectively and the current decreases as discussed above. The current suppression is complete once both transitions $0_q \to 1_{q+1}$ and $1_q \to 0_{q+1}$ are allowed.

(d) Absorption by incoming electrons. In Fig. 13 resonances $\mu_L = \mu_{-k}^2, k = 1, 2$ (negative slope) are visible which correspond to absorption of the vibrational energy by an incoming electron ($2_q \leftarrow 0_{q+k}$). What is remarkable compared to Fig. 12 is that the current *decreases* here. This is another signature of the population inversion due to the feedback mechanism. Vibrational energy can accumulate on the molecule through previous sequences of tunneling events involving only the weakly coupled orbital 1. The molecule is then "brought to a standstill" when, in a single tunneling process, an electron with an energy deficit matching the total accumulated vibrational energy enters: $2_0 \leftarrow 0_k$. For $\mu_k^2 < \mu_L < \mu_0^2$ there are $[\Delta/\omega]$ such resonance lines where

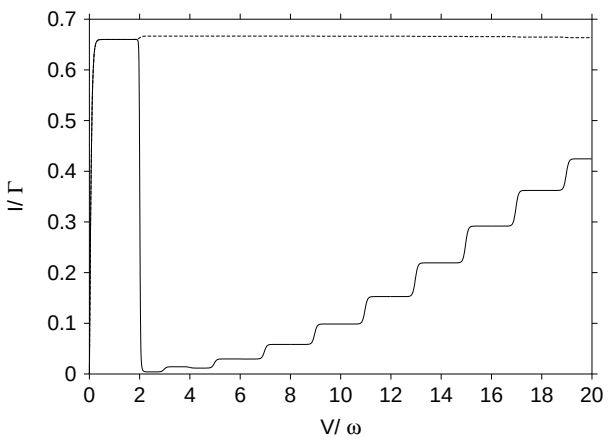


FIG. 15: $I(V)$ for $\mu - \mu_0^1 = 0.0$ in Fig. 13 for non-equilibrium (full, Eq. (7)) and equilibrium vibrations (dashed, Eq. (14)). The current plateau is caused by the weakly coupled ground state 1. The current suppression is due to the strongly coupled excited state 2 at $\Delta = 2.5\omega$ which is only accessible by a *single*-electron tunneling process for $V > 5.0\omega$ (cf. Fig. 8). However, a cascade of such processes, whereby vibrational energy accumulates on the molecule, allows this state to become occupied already at low V, Figs. 14(b),(c).

such a new trapping process becomes possible. Note that this can not be understood as an effect of heating since at these resonances the occupation of vibrational excited states is suppressed due to the feedback and the current is reduced.

Intermediate relaxation. Compared with Section II B 2 the non-equilibrium effects are more sensitive to relaxation since here roughly $2\Delta/\omega$ tunneling events comprise the feedback mechanism instead of 2 (cf. Figs. 9 and 14). This restricts the minimal vibrational quality factor $\mathcal{Q}$ (writing the vibrational relaxation rate as $\gamma = \omega/\mathcal{Q}$, cf. Sec. I) for the observation of effects due the feedback mechanism to $\mathcal{Q} > 2\Delta/\omega$ for $\lambda_1^2 \ll 1 \ll \lambda_2^2$. In contrast, for $\lambda_1^2 \gg 1 \gg \lambda_2^2$ the requirement is $\mathcal{Q} > 2$. For the cases discussed here only $\mathcal{Q} \gg 5$ is required. This is confirmed by our calculations for intermediate values of the relaxation rate γ. Interestingly, when increasing the vibrational relaxation rate γ starting from zero, the dependence of the amplitude NDC line with positive slope $\mu_R = \mu_1^1$ (proof of a non-equilibrium distribution) is non-monotonic: it is initially weakened and then regains amplitude and remains clearly visible with increasing γ. Also the current peak shifts to larger values of $\mu - \mu_0^1$ and V but remains visible. The low-bias effects of the excited state are however suppressed since cascades responsible for the population inversion effect are cut off by the relaxation.

In summary, it is remarkable that in all discussed cases (a)-(d) the excited state 2_0 dominates the current at low bias where it can not be reached from the neutral ground state 0_0 by a single-electron tunneling process. The strong deviation from equilibrium is induced by cascades of single electron tunneling processes.

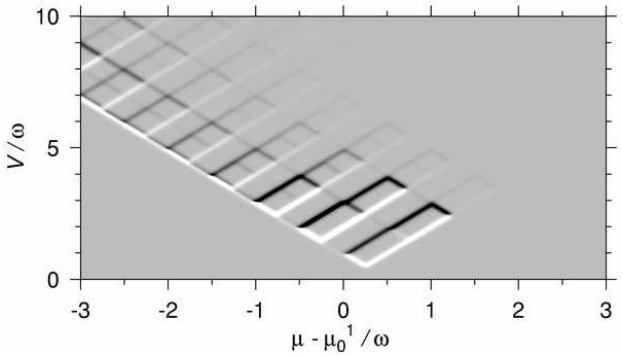


FIG. 16: $dI/dV(\mu, V)$ for $\lambda_1 = 5.0$, $\lambda_2 = 1.1$ and $\Delta/\omega = 0.5$.

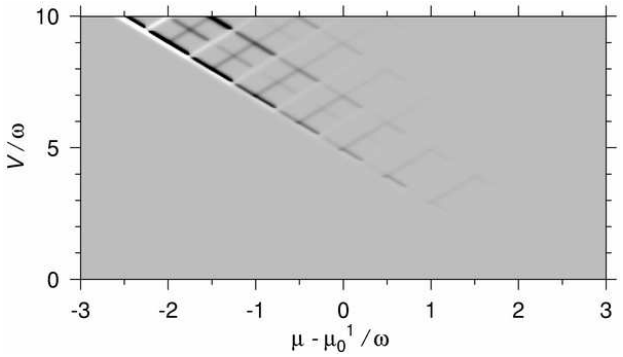


FIG. 17: $dI/dV(\mu, V)$ for $\lambda_1 = 5.0$, $\lambda_2 = 1.1$ and $\Delta/\omega = 2.5$.

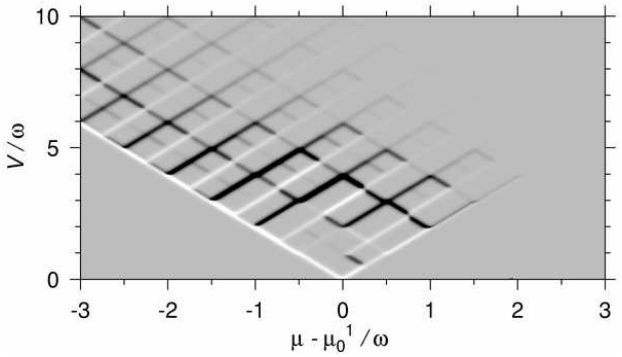


FIG. 18: $dI/dV(\mu, V)$ for $\lambda_1 = 1.1$, $\lambda_2 = 5.0$ and $\Delta/\omega = 0.5$.

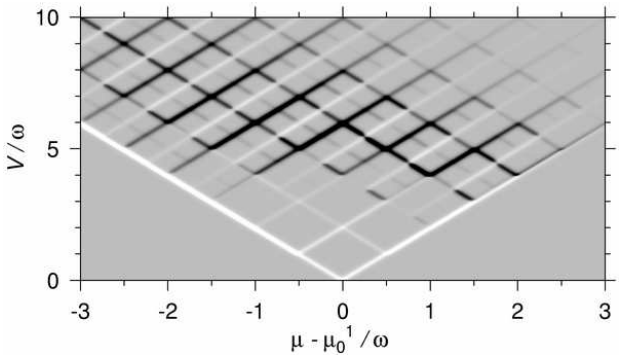


FIG. 19: $dI/dV(\mu, V)$ for $\lambda_1 = 1.1$, $\lambda_2 = 5.0$ and $\Delta/\omega = 2.5$.

D. Non-degenerate strongly coupled states

Having analyzed the above cases in detail, we can now restrict ourselves to a brief classification of the results for non-degenerate states $\Delta > 0$ where both $\lambda_1^2 \neq \lambda_2^2 > 1$. Here the feedback mechanism discussed above produces more complex results. The basic change is that when the *weakest* coupling is increased the feedback mechanism becomes less efficient at populating vibrational excitations of the neutral molecule (compare with the feedback mechanism for a single orbital Sec. II A). More vibrational excitations of the weakly coupled orbital and the neutral state must be accessible by a single tunneling process in order to fully activate the feedback and trap the molecule in *strongest* coupled orbital. The patterns of NDC lines will therefore extend over a broader range of applied voltages. Indeed, a glance at Figs. 16-19 already shows that more NDC lines are visible. Also, there are more NDC lines with positive slope, which proves that the deviations from an equilibrium vibrational distribution are stronger. For $\lambda_1^2 \gg \lambda_2^2 > 1$ the NDC effects are strongest for the case $\Delta < \omega$ presented in Fig. 16. Compared with Fig. 8 the isolated region defined by strong NDC lines is repeated a number of times to the left and it extends further to the right. Also, the current peak at the resonance line $\mu_L = \mu_0^2$ has shifted further to the left. The extended $I(V)$ plateaus have a width fixed by $\omega - \Delta$, independent of the gate voltage (compare with the weak NDC in Sec. II B 1 where the current steps and drops have opposite gate-voltage dependence). For the case $\Delta > \omega$ presented in Fig. 17 the low bias structure disappears and the current peak along $\mu_L = \mu_0^2$ becomes the dominant feature. For $\lambda_2^2 \gg \lambda_1^2 > 1$ the NDC effects are strongest for the case $\Delta > \omega$ presented in Fig. 19. The two strong NDC lines in Fig. 13 have developed into a "checkerboard" pattern of such lines. These correspond to excitations of the weaker coupled state. In addition more resonances due to the strongly coupled state appear. For $\Delta < \omega$ the current is more suppressed at positive gate energies, Fig. 18.

III. SUMMARY AND DISCUSSION

We have calculated the non-linear current through a molecule with two non-degenerate electron-accepting orbitals coupled asymmetrically to an internal vibration in the limit of weak tunneling to the electrodes. We found that due to the interplay of Coulomb blockade and non-equilibrium vibration-assisted tunneling NDC effects become amplified and pervasive in comparison with a one-orbital model. The only resonances where we consistently find current steps correspond to an electron tunneling off the molecule starting from the charged state coupled strongly to the vibration. At all other resonance lines the dI/dV may become negative depending on the electron-

vibration couplings and applied voltages. A weak and strong NDC effect may be distinguished, which require the larger of the two electron-vibration couplings to be moderate and strong respectively.

The weak NDC effect is found at resonance lines where an electron can tunnel onto the molecule resulting in the charged state coupled *stronger* to the vibration. This effect only occurs when two (or more) orbitals are competing in the transport. The current steps and drops occur at bias positions with an *opposite* gate-voltage dependence and give rise to current *oscillations*. We proved that this type of NDC is robust against strong relaxation of the vibrational distribution on the molecule due to a dissipative environment. Any NDC at other resonances conditions is a proof of a non-equilibrium vibrational distribution on the molecule. The current oscillations may even become amplified by strong relaxation depending on the applied voltages.

Strong NDC effects appear at the first few resonance lines associated with the state *weakly* coupled to the vibration. This is a non-equilibrium effect which is typically weakened by relaxation processes. Cascades of single-electron tunneling processes involving the vibrational excitations of the weakly coupled state provide a *feedback* which rapidly populates the strongly coupled state. The latter thus acts as a blocking state which is almost fully occupied. The few, strong NDC lines correspond to the activation of the feedback mechanism and can have the *same* gate voltage dependence as the current steps, in contrast to the weak NDC above. In a one-orbital model the feedback mechanism is also active but produces only a weak effect due to the absence of a competing orbital. An anomalous *current peak* of width $\propto T$ appears when the feedback mechanism becomes effective only sufficiently deep *inside* a resonance. The peak signals the crossover of the vibrational distribution from equilibrium to non-equilibrium.

Interestingly, the blocking state can be the vibrational ground state of either charged state whichever couples stronger to the vibration. When the electronic excited orbital couples most strongly the NDC signals a voltage-controlled *population inversion* between the charged states induced by the vibration-assisted tunneling. Also, new resonances appear associated with an electron entering the molecule and *absorbing* vibrational energy stored on it (despite the low temperature) where the current is *suppressed*.

The NDC effects are due to asymmetry of the orbital energies and couplings to the internal vibration which are *intrinsic* properties of the molecule. One can thus tailor the electronic response of the device by molecular engineering. In contrast to other NDC effects, we do not require detailed assumptions of orbital- and/or electrode- specific electronic wave-function overlap with the electrodes [19, 25, 33, 34] nor bias-voltage dependent coupling to the vibration [12].

For the interpretation of transport spectroscopy experiments on molecular devices an important result of our work is that multiple orbitals may be relevant for effects at voltages where only a single orbital would seem to matter. For instance, an excited orbital may already dominate the transport by cascades of single tunneling events at a low voltage where this state is not directly accessible from the neutral ground state, cf. Fig. 13. Similarly the charged ground state may completely dominate the transport even at a high bias voltage where a far "better conducting" excited orbital is already directly accessible cf. Fig. 8.

We have used a basic parameterization of the nuclear potential surface of the electronic states and some comments are appropriate. For one, the nuclear potential shape may be anharmonic in the coordinate Q considered here. The resulting qualitative changes may be determined from the FC-factors for these potentials, when plotted in similar fashion as Fig. 2. The main results are not sensitive to the fine details of these factors but only to their large-scale dependence on the vibrational numbers due to the shift of the potentials, which can be established by quasi-classical considerations. Secondly, anharmonic terms in the nuclear potential may also couple the mode Q to other internal modes which we have not considered here. When this coupling is strong for a large number of such other modes or a Fermi- (nonlinear-)resonance is involved, intramolecular vibrational energy redistribution may relax the vibration. Generally, this will become more important for large molecules. The effect of relaxation has been discussed. If however, only a few other modes couple strongly to Q, say one, an interesting two mode problem occurs. A treatment of the effects of such multi-mode dynamics [21] on the tunneling transport, lies outside the scope of the present paper.

Acknowledgments

We acknowledge stimulating discussions with H. Schoeller, K. Flensberg, W. Belzig, I. Sandalov, and M. Hettler. M. R. W. acknowledges the financial support provided through the European Community's Research Training Networks Program under contract HPRN-CT-2002-00302, Spintronics.

APPENDIX A: STRONG RELAXATION

We consider the limit $\Gamma \ll \gamma \ll T$ where the vibrational excitations have completely relaxed before each tunneling event due to a dissipative environment. The tunneling rates Γ^{ir} are not assumed to be symmetric. With the factorization ansatz $P^i_q = P^i P_q$, $P_q = e^{-q\omega/T}(1 - e^{-\omega/T})$ we can reduce equations (4) to an effective electronic three-level problem with voltage dependent rates (13). The stationary probabilities and the

current can be explicitly given ($r = R, L$):

$$\frac{P^i}{P^0} = 2\frac{W_{i\leftarrow 0}}{W_{0\leftarrow i}}, P^0 = \left[1 + 2\sum_i \frac{W_{i\leftarrow 0}}{W_{0\leftarrow i}}\right]^{-1}, \quad \text{(A1)}$$

$$I_r = \sum_i \left(2W^r_{i\leftarrow 0}P^0 - W^r_{0\leftarrow i}P^i\right). \quad \text{(A2)}$$

We can now find a simple explicit condition for the occurrence of current steps or drops with increasing bias voltage. Consider an increase of the positive bias $V \to V'$ such that one additional transition involving orbital i comes into the bias window through a resonance with electrode $r = L, R$, $\mu_r = \mu^i_k$ for some $k = 0, \pm 1, \pm 2, \ldots$ (for $V < 0$ interchange $L \leftrightarrow R$ below). For simplicity we consider the values of the current on the two subsequent plateaus: only two transition rates are then changed, $W_{i\leftarrow 0} \to W'_{i\leftarrow 0}$ and $W_{0\leftarrow i} \to W'_{0\leftarrow i}$ the changes being related by $\delta W^r_{0\leftarrow i} = -e^{-k\beta\omega}\delta W^r_{i\leftarrow 0}$ (cf. Eqs. 5, 13). The change in the stationary current $\delta I_r = I'_r - I_r$ may be calculated at either electrode $r = L, R$ from (14) (since $I_L + I_R = I'_L + I'_R = 0$):

$$\frac{\delta I_r}{I_r} = 2\left(\frac{W'_{i\leftarrow 0}}{W'_{0\leftarrow i}} - \frac{W_{i\leftarrow 0}}{W_{0\leftarrow i}}\right)P'^0\left(\frac{W^{\bar r}_{0\leftarrow i}}{I^r} - 1\right), \quad \text{(A3)}$$

Here $\bar r = R, L$ denotes the electrode opposite to $r = L, R$. In order to have NDC at a resonance where μ_L becomes larger than μ^i_k we require $\delta I_L/I_L < 0$, which, using $r = L$ in Eq. (A3), gives $W^R_{0\leftarrow i} - I_L < 0$. The rate of escape through junction R at voltage V' (including the new transition in increased bias window V') must thus be smaller than the current I_L at initial voltage V. It is readily seen that this condition cannot be fulfilled in the case of only one orbital: $W^R_{0\leftarrow 1} - I_L = W^R_{0\leftarrow 1} + I_R = 2W^R_{1\leftarrow 0}P^0 + W^R_{0\leftarrow 1}(1 - P^1) > 0$. However, for two (or more) orbitals it is possible to satisfy this requirement. To see if NDC may occur at a resonance where μ_R drops below μ^i_k we use $r = R$ in Eq (A3), leading to the requirement $W^L_{0\leftarrow i} - I_R = W^L_{0\leftarrow i} + I_L < 0$. which can not be satisfied for any applied voltages since $I_L > 0$ for $V > 0$. The current *must* increase at such resonances. Thus for fully equilibrated vibrations NDC can only occur at resonances related to the left electrode, $\mu_L = \mu - \mu^i_k, k = 0, \ldots$, where electrons can enter the molecule by an additional tunneling process $i_{q+k} \leftarrow 0_q$. These resonances correspond to lines with positive slope in the (μ, V) plane. Any NDC occurring at an other resonance is a proof of a non-equilibrium vibrational distribution. This proof can be trivially extended to N orbitals correlated by Coulomb charging (maximally one extra electron). It also does not depend on the FC-factors involved, although the amplitude of the possible NDC may be small for a particular choice.

APPENDIX B: UNCORRELATED VIBRATION-ASSISTED TUNNELING

We consider the special case where the renormalization of the interaction (due to the polaron effect) compensates the Coulomb repulsion effects, i.e. $v = v^{(0)} - 2\omega\lambda_1\lambda_2 = 0$. Now we have to include the doubly charged state of the molecule $n_1 = 1, n_2 = 1$ (di-anion). We denote the diagonal density matrix elements by $P^{n_1n_2}_q$, where q is the vibrational number and n_1n_2 denotes an electronic state with occupations $n_i = 0, 1$ of orbital $i = 1, 2$. The occupations are coupled by the stationary master equations (cf. [35])

$$-\sum_i \left[n_i \sum_{q'} W_{0q'\leftarrow iq} + (1 - n_i)\sum_{q'} 2W_{iq'\leftarrow 0q}\right] P^{n_1n_2}_q$$
$$+\sum_{q'}\Big[2n_1 W_{1q\leftarrow 0q'}P^{0n_2}_{q'} + 2n_2 W_{2q\leftarrow 0q'}P^{n_10}_{q'}$$
$$+(1 - n_1)W_{0q\leftarrow 1q'}P^{1n_2}_{q'} + (1 - n_2)W_{0q\leftarrow 2q'}P^{n_11}_{q'}\Big] = 0$$

together with $\sum_{n_1n_2} P^{n_1n_2} = 1$. In the case where the vibration is assumed to be completely equilibrated, $\bar P^{n_1n_2}_q = \bar P^{n_1n_2}P_q$ the kinetic equations can be decoupled into equations for the occupations of two uncorrelated "channels", $\bar P^i \equiv \sum_{n_1n_2}\delta_{1n_i}P^{n_1n_2}$ with the rates (13): $\bar P^i = 0 = 2W_{i\leftarrow 0}(1 - \bar P^i) - W_{0\leftarrow i}\bar P^i$. The current is then a sum of independent contributions of the individual orbitals: $I_r = \sum_i I_{ri}$ where $I_{ri} = ({W^r_{0\leftarrow i}}^{-1} + 2{W^r_{i\leftarrow 0}}^{-1})^{-1}$. For a single orbital the current monotonically increases in the limit of strong relaxation (Appendix A) and the same thus holds for two (or more) uncorrelated orbitals.

[1] G. Herzberg, *Molecular spectra and molecular structure* (Van Nostrand, 1950).

[2] L. Kouwenhoven, C. Marcus, P. McEuen, S. Tarucha, R. Westervelt, and N. Wingreen, *Mesoscopic Electron Transport* (Kluwer, 1997), p. 105.

[3] H. Park, J. Park, A. K. L. Lim, E. H. Anderson, A. P. Alivisatos, and P. L. McEuen, Nature **407**, 52 (2000).

[4] J. Park, A. N. Pasupathy, J. I. Goldsmith, C. Chang, Y. Yaish, J. R. Petta, M. Rinkoski, J. P. Sethna, H. D. Abruña, P. L. McEuen, et al., Nature **417**, 722 (2002).

[5] A. N. Pasupathy, J. Park, C. Chang, A. V. Soldatov, S. Lebedkin, R. C. Bialczak, J. E. Grose, L. A. K. Donev, J. P. Sethna, D. C. Ralph, et al., Nano Lett. **5** (2005).

[6] L. H. Yu, Z. K. Keane, J. W. Ciszek, L. Cheng, M. P. Stewart, J. M. Tour, and D. Natelson, Phys. Rev. Lett. **93**, 266802 (2004).

[7] L. H. Yu and D. Natelson, Nanotechnology **15**, S517 (2004).

[8] L. H. Yu and D. Natelson, Nano Lett. **4**, 79 (2004).

[9] S. Braig and K. Flensberg, Phys. Rev. B **68**, 205324 (2003).

[10] S. Braig and K. Flensberg, Phys. Rev. B **70**, 085317 (2004).

[11] D. Boese and H. Schoeller, Eur. Phys. Lett. **54**, 668

(2001).
[12] K. D. McCarthy, N. Prokofev, and M. T. Tuominen, Phys. Rev. B **67**, 245415 (2003).
[13] A. Mitra, I. Aleiner, and A. J. Millis, Phys. Rev. B **69**, 245302 (2004).
[14] J. Koch, M. Semmelhack, F. von Oppen, and A. Nitzan, cond-mat/0504095.
[15] J. Koch and F. von Oppen, Phys. Rev. Lett. **94**, 206804 (2005).
[16] J. Koch, M. Raikh, and F. von Oppen, cond-mat/0501065.
[17] P. S. Cornaglia, H. Ness, and D. R. Grempel, PRL **93**, 147201 (2004).
[18] P. S. Cornaglia, H. Ness, and D. R. Grempel, cond-mat/0409021.
[19] M. H. Hettler, W. Wenzel, M. R. Wegewijs, and H. Schoeller, Phys. Rev. Lett. **90**, 076805 (2003).
[20] G. A. Kaat and K. Flensberg, cond-mat/0411173.
[21] H. Koeppel, W. Domcke, and L. S. Cederbaum, Adv. Chem. Phys. **57**, 59 (1984).
[22] M. Cizek, M. Thoss, and W. Domcke, cond-mat/0411064.
[23] I. G. Lang and Y. A. Firsov, Sov. Phys. JETP **16**, 1301 (1963).
[24] J. Koch, F. von Oppen, Y. Oreg, and E. Sela, cond-mat/0405453.
[25] M. Hettler, H. Schoeller, and W. Wenzel, *Nano-Physics and Bio-Electronics: A New Odyssey* (Elsevier, Amsterdam, 2002), pp. 303–322.
[26] A. Thielmann, M. H. Hettler, J. König, and G. Schön, cond-mat/0406647 (2004).
[27] A. Cottet, W. Belzig, and C. Bruder, Phys. Rev. Lett. **92**, 206801 (2004).
[28] A. Cottet, W. Belzig, and C. Bruder, Phys. Rev. B **70**, 115315 (2004).
[29] W. Belzig, Phys. Rev. B **71**, 161301(R) (2005).
[30] A. Perelomov, *Generalized Coherent States and Their Applications* (Springer-Verlag, Berlin, 1986).
[31] D. Weinmann, W. Häusler, and B. Kramer, Phys. Rev. Lett. **74**, 984 (1995).
[32] C. Romeike, M. R. Wegewijs, and H. Schoeller, cond-mat/0502091.
[33] M. Hettler, H. Schoeller, and W. Wenzel, Eur. Phys. Lett. **57**, 571 (2002).
[34] A. Thielmann, M. H. Hettler, J. König, and G. Schön, Phys. Rev. B **68**, 115105 (2003).
[35] M. R. Wegewijs and Y. V. Nazarov, Phys. Rev. B **60**, 14318 (1999).